Calculation of viscous EHL traction for squalane using molecular simulation and rheometry

Scott Bair[a], Clare McCabe[b] and Peter T. Cummings[c]

[a]Center for High-Pressure Rheology, George W. Woodruff School of Mechanical Engineering, Georgia Institute of Technology, Atlanta, GA 30332-0405

[b]Department of Chemical Engineering, Colorado School of Mines, Golden, CO 80401

[c]Departments of Chemical Engineering, Chemistry and Computer Science, University of Tennessee, Knoxville TN 37996-1508 and Chemical Sciences Division, Oak Ridge National Laboratory, Oak Ridge TN 37831

Received May 26, 2002; accepted August 9, 2002

Recently, remarkable agreement was reported between nonequilibrium molecular dynamics simulation and high-pressure Couette rheometry on squalane. We have utilized the viscosity-strain rate relationship obtained from this unique combination of experimental and simulation data along with high-pressure viscometer measurements to calculate the viscous traction curve in the elastohydrodynamic lubrication (EHL) regime. A comparison with measured traction at 0.57 and 1.29 GPa shows excellent agreement, confirming the validity of the measurements and simulations. Thus, we present for the first time, a successful calculation of EHL traction from the liquid shear response obtained from both molecular dynamics and rheometry.

KEY WORDS: EHL traction; high-pressure rheology; shear-thinning; nonequilibrium molecular dynamics simulation; elastohydrodynamics

1. Introduction

The calculation of traction in the elastohydrodynamic lubrication (EHL) regime from the properties of the lubricant has been an elusive goal of tribology for at least forty years. Traction is usually represented by a plot of the traction force, average shear stress or traction (friction) coefficient against the sliding velocity, slide-to-roll ratio or average shear rate, often on a logarithmic scale. Traction is important to the designer of cams, gear trains and rolling bearings because it characterizes the mechanical loss to the system. Also, the traction properties of candidate fluids may determine the feasibility of toroidal continuously variable automobile transmissions (also known as traction drives).

Investigations have followed two general methodologies: In the first, the traction curve itself is regarded as a rheological flow curve and the pressure-averaged rheological properties are extracted directly from the traction curve. See [1] for an example. Of course, this method leads to a precise reconstruction of the traction curve; however, the properties obtained from this curve (including the viscosity-strain rate relation) do not agree with the same properties measured directly in other apparatuses (referred to as out-of-contact measurements) and are not useful for calculation of film thickness [2]. The second method requires that properties and constitutive behavior be measured out-of-contact. Traction is then calculated by integration over the contact area with pressure-dependent properties. See [3] for an example. The constitutive and property relations derived for this approach are useful for calculations of film thickness [4] as well. This second method is adopted here.

In related prior work, Chynoweth *et al.* [5] performed constant-volume nonequilibrium molecular dynamics simulations on two C_{16} hydrocarbon liquids. The results were fitted to the empirical Cross equation to describe the relationship between viscosity and shear rate. A pressure-viscosity relation was assumed and traction curves were computed for the Cross equation with a numerical EHD solver. At the time, it was necessary to adjust parameters to achieve reasonable traction curves and there was no comparison with experimentally measured traction.

Recently, remarkable agreement has been reported between nonequilibrium molecular dynamics (NEMD) simulations and high-pressure Couette rheometry for the branched C_{30} hydrocarbon squalane (2,6,10,15,19,23-hexamethyltetracosane) [6]. The NEMD simulations predict shear-thinning behavior at high strain rates due to the alignment of the squalane molecules with the imposed planar Couette flow field. A master curve, figure 1, was constructed using the standard form of time-temperature-pressure superposition, and the Carreau fit shown in figure 1 is used in this work to calculate a traction curve for squalane. The result compares well with experimentally measured traction for the same liquid. Thus, we present for the first time a successful

1023-8883/02/1100-0251/0

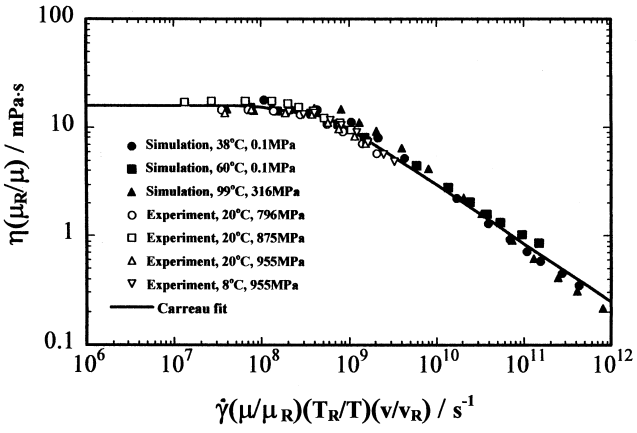

Figure 1. Master flow curve constructed from nonequilibrium molecular dynamics simulation and high-pressure Couette rheometry.

calculation of EHL traction from the liquid shear response obtained from both molecular dynamics and rheometry.

2. Simulations

The calculations used to generate the simulation results shown in figure 1 were obtained by non-equilibrium molecular dynamics (NEMD) simulation, a particularly useful technique for studying rheological properties, since the key algorithm (SLLOD) [7] is a direct implementation of the experimental method for measuring viscosity and because it can also be used to probe the non-Newtonian regime, common to polymers and other high-molecular-weight systems, in which the transport properties are nonlinear in the applied field. The NEMD SLLOD algorithm for viscosity involves applying a planar Couette flow field at strain rate $\dot{\gamma} = \mathrm{d}u_x/\mathrm{d}y$, which characterizes the constant change in streaming velocity u_x in the horizontal x direction with vertical position y. The viscosity at strain rate $\dot{\gamma}$ is then computed from

$$\eta = -\frac{\left\langle P_{xy}^{0,s} \right\rangle}{\dot{\gamma}} \tag{1}$$

where $P_{xy}^{0,s}$ is the traceless symmetrized pressure tensor computed in the course of the simulation. The result is the strain-rate dependent shear-thinning viscosity shown in reduced units in figure 1. Further details on the simulation results can be found in references [6,8,9].

3. Experimental

We have measured the traction of squalane at 40 °C in elliptical contact using a skewed roller traction rig similar to that described by Poon [10] with a contact aspect ratio of 1.61. The hardened steel rollers were produced with a composite arithmetic average roughness of 21 nm. The traction data are plotted as points in figure 2 for Hertz pressure of $p_H = 1.29$ GPa and rolling velocity of $U = 2$ m/s and film thickness of $h = 177$ nm. The contact radius in the rolling direction is $a = 1.2 \times 10^{-4}$m.

The limiting low shear viscosity, μ, has been obtained to a pressure of 1.06 GPa with falling-body viscometers. The relative volume to 0.42 GPa has been measured in a bellows piezometer. These data are listed in table 1. The constitutive behavior of squalane has been thoroughly characterized by NEMD and high-pressure Couette rheometry resulting in published [6] values of the Carreau parameters and a validation of standard time-temperature-pressure shifting rules for this liquid. Descriptions of the viscometers and the piezometer with estimated accuracies and comparisons with other pub-

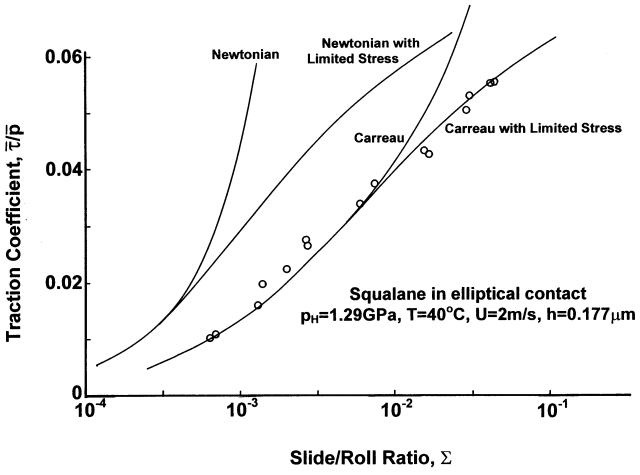

Figure 2. Traction measured in high-pressure elliptical concentrated contact presented as circles and calculations presented as curves. $\Lambda = 0.075$.

Table 1
Measured properties of squalane.

p/MPa	40 °C		30 °C
	v/v_o	μ/Pa · s	μ/Pa · s
0.1	1	0.0154	0.0225
34.5	0.976	0.0301	–
69	0.957	0.0554	0.0957
146	0.928	0.183	0.351
224	0.905	0.544	0.961
301	0.887	1.55	2.90
378	0.870	4.01	7.35
424	0.862	–	
467		8.56	
586		29.0	
705		83.0	
823		259	
942		829	
1060		2780	

lished data may be found in [11]. The rheometer is described in [12].

4. Traction Calculations

The calculation presented here assumes viscous response of the lubricant film. To show that a viscous calculation is acceptable we calculate the Deborah number, $\mathrm{De} = \mu U/G_\infty a$, where G_∞ is the limiting high rate shear modulus that may be estimated from ultrasonic measurements [13] to be about 2 GPa at the average contact pressure. The viscosity here is about $\mu = 1000\ \mathrm{Pa}\cdot\mathrm{s}$ giving $\mathrm{De} = 0.008$. For low De, the elastic response of the film may be neglected. Also, the theoretical linear traction gradient due to steel compliance [14] is $1.78G_s/P_H = 110$, where G_s is the shear modulus of steel. The Newtonian traction gradient is $U\mu/\bar{p}h \approx 12$ so that steel compliance may be neglected. The steel rollers are stiffer than the film.

We represent the variation of low shear viscosity with pressure by the Doolittle [15] equation:

$$\mu(p) = \mu_0 \exp\left[B\,\frac{v_{\mathrm{occ}}\,(v_0 - v)}{(v - v_{\mathrm{occ}})(v_0 - v_{\mathrm{occ}})}\right] \tag{2}$$

where v is volume, v_0 is volume at $p = 0$, and v_{occ} is the occupied volume, independent of pressure. The variation of volume with pressure is described with the Tait equation [15]:

$$v/v_0 = 1 - \frac{1}{K_0'+1}\ln\left[1+\frac{p}{K_0}\left(1+K_0'\right)\right]. \tag{3}$$

A least-squares regression of volume and viscosity data together resulted in $K_0 = 0.907\,\mathrm{GPa}$, $K_0' = 13.7$, $v_{\mathrm{occ}}/v_0 = 0.669$ and $B = 4.10$ with $\mu_0 = 12.9\,\mathrm{mPa}\cdot\mathrm{s}$ regarded as an adjustable parameter.

We represent the constitutive behavior by the shifted Carreau equation for viscosity:

$$\eta(\dot{\gamma},\, p) = \mu\left[1 + \left(\dot{\gamma}\lambda_{\mathrm{R}}\,\frac{\mu}{\mu_{\mathrm{R}}}\,\frac{T_R}{T}\,\frac{v}{v_R}\right)^2\right]^{(n-1)/2} \tag{4}$$

where μ_R and λ_R are the low shear viscosity and the relaxation time at $T_R = 311\,\mathrm{K}$ (38 °C) and ambient pressure and $\dot{\gamma}$ is shear rate. From published [6] NEMD and experimental measurements, $\mu_{\mathrm{R}} = 15.6\,\mathrm{mPa}\cdot\mathrm{s}$, $\lambda_{\mathrm{R}} = 2.26\times10^{-9}\mathrm{s}$ and $n = 0.463$. For v/v_R we substitute v/v_0 from equation (3) and μ is calculated from equation (2).

The Newtonian limit in terms of shear stress is, from equation (4), always greater than 1.5 MPa. Therefore, a Newtonian inlet-zone film-thickness calculation is appropriate and the Dowson–Hamrock [16] formula for central film thickness was used to arrive at $h = 0.177\ \mu\mathrm{m}$. The film thickness in EHL is established in the inlet zone upstream or ahead of the Hertz contact region where the greater part of the traction is generated. The shear rate in the Hertz region can be calculated from

$$\dot{\gamma} = \frac{U\Sigma}{h} \tag{5}$$

where Σ is the contact slide to roll ratio, assuming a uniform value of h over the Hertz contact area.

The average contact shear stress results from integration of the local stress, τ, over the contact area,

$$\bar{\tau} = \int_0^1 2r\tau\ \mathrm{d}r \tag{6}$$

for dimensionless contact radius, $0 < r < 1$. For point contact the average pressure is $\bar{p} = 2/3\,p_H$ and the traction coefficient is simply $\bar{\tau}/\bar{p}$. We assume that the pressure distribution is identical to that of the unlubricated Hertz contact:

$$p = p_H\left(1 - r^2\right)^{1/2}. \tag{7}$$

First, we calculate traction for the Newtonian and Carreau cases where

$$\tau = \mu(p)\dot{\gamma} \tag{8}$$

and

$$\tau = \eta(p,\dot{\gamma})\dot{\gamma} \tag{9}$$

respectively. The traction curves for these cases are indicated in figure 2.

We know from experimental measurement that at sufficiently large shear stress, τ, relative to the pressure, p, the deformation will localize within the film, limiting the magnitude of the shear stress. This has been shown in experimental flow visualization [17] and has been examined by molecular simulation [18]. Gray *et al.* [18] performed NEMD simulations of a model fluid (each molecule consisted of two monatomic particles connected by a spring) and demonstrated that shear localization could occur at high strain rate, providing a possible explanation for limiting shear stress. However, techniques for themostatting molecular fluids at high strain rate are the subject of some controversy [19], and so their conclusions are subject to confirmation by more careful studies with other, more rigorous thermostatting mechanisms such as those based on the configurational temperature [20]. In this work, we assume a limiting shear stress but do not attempt to probe its molecular basis. The ratio of $\tau/p = \Lambda$ that limits the shear stress was found from a traction measurement at $p_H = 1.93\,\mathrm{GPa}$ where the traction coefficient reached a plateau at 0.075. For this high pressure the Deborah number is not small and the initial traction gradient is comparable to the theoretical traction gradient for steel compliance, precluding a viscous traction calculation. However, the value of Λ can be utilized to extend our calculated traction curve. Two additional curves are plotted in figure 2 for Newtonian response with limiting

shear stress

$$\tau = \min[\mu\dot{\gamma}, \Lambda p] \tag{10}$$

and Carreau behavior with limiting stress

$$\tau = \min[\eta\dot{\gamma}, \Lambda p] \tag{11}$$

with $\Lambda = 0.075$.

As shown in figure 2, Carreau behavior captures the low sliding speed traction very well and with a limit to the shear stress it describes all of the measured traction. We also find that using different values of $\Lambda = 0.065$ or 0.085 does not fit the measured traction data as well as the value obtained from the traction plateau.

Additional traction measurements are available for squalane for low pressure and somewhat reduced temperature from Stejskal and Cameron [21]. A circular point contact between a steel ball and a glass disc was used to generate the data shown in figure 3 for $T = 37\,^{\circ}\mathrm{C}$ and Hertz pressure, $p_H = 0.57\,\mathrm{GPa}$. Additional viscosity measurements were performed at 30 °C and are listed in table 1. The temperature-viscosity coefficient was assumed to be constant over the interval from 30 to 40 °C and a correction was made to the viscosity calculated by equation (2) for the lower temperature. This correction increased the viscosity by about 18%. The density increase for the lower temperature was neglected.

The resulting traction curve for the Carreau equation is shown to agree with measurements in figure 3. Limiting the stress by $\Lambda = 0.075$ did not alter the result. For this very low pressure contact, the shear stress does not reach a significant fraction of the pressure locally.

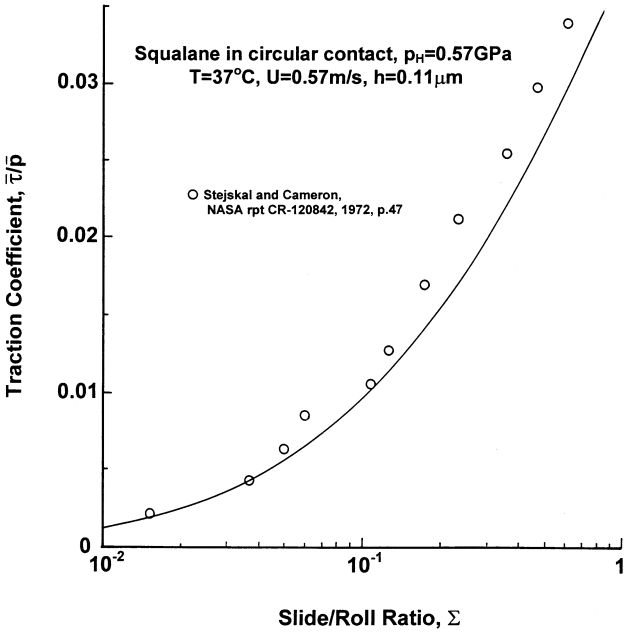

Figure 3. Traction measured in low-pressure circular contact from reference [21] presented as circles and calculation presented as the curve.

5. Conclusion

Using the viscosity-strain rate relation obtained previously from a combination of NEMD simulations and experimental measurements, we have successfully calculated the elastohydrodynamic viscous traction curve. A comparison with measured traction at 1.29 and 0.57 GPa shows excellent agreement, confirming the validity of the measurements and simulations. Thus, we present for the first time, a successful calculation of EHL traction from the liquid shear response obtained from molecular dynamics and rheometry. It is important to recognize that without the availability of both the simulation and experimental data, leading to the parametrization of the Carreau curve over a wide range of strain rate—including the non-Newtonian shear-thinning regime—this would not have been possible.

References

[1] W. Hirst and A.J. Moore, Proc. R. Soc. Lond. A365 (1979) 537.
[2] A. Dyson and A.R. Wilson, Proc. Instn. Mech. Engrs. 180 (3K) (1965—6) 97.
[3] S. Bair, in: *Tribology Research: From Model Experiment to Industrial Problem*, eds. G. Dalmaz, *et al.* (Elsevier, Amsterdam, 2001) p. 733.
[4] J.A. Greenwood and J.J. Kauzlarich, Proc. Instn. Mech. Engrs., 212(J3) (1998) 179.
[5] S. Chynoweth, R.C. Coy, A.J. Holmes and L.E. Scales, *Elastohydrodynamics '96* (Elsevier, 1997) p. 261.
[6] S. Bair, C. McCabe and P.T. Cummings, Phys. Rev. Lett. 88(5), (2002), pp. 058302-1.
[7] D.J. Evans and G.P. Morriss, Phys. Rev. A 30, (1984) 1528.
[8] J.D. Moore, S.T. Cui, H.D. Cochran, P.T. Cummings and J. Chem. Phys. 113 (2000) 8833.
[9] C. McCabe and P. T. Cummings, in preparation (2002).
[10] S.Y. Poon and D.J. Haines, Proc. Instn. Mech. Engrs. 181(1) (1966) 363.
[11] S. Bair, J. Jarzynski and W.O. Winer, Tribol. Intrn. 34 (2001) 461.
[12] S. Bair, Proc. Instn. Mech. Engrs. 216 (J) 139.
[13] G. Harrison, *The Dynamic Properties of Supercooled Liquids* (Academic Press, London, 1976), p. 143.
[14] K.L. Johnson and J.L. Tevaarwerk, Proc. R. Soc. Lond. A356 (1977) 215.
[15] R.L. Cook, H.E. King, C.A. Herbst and D.R. Herschbach, J. Chem. Phys., 100(7) (1994) 5178.
[16] B.J. Hamrock, *Fundamentals of Fluid Film Lubrication* (NASA RP1255, 1991) p. 475.
[17] S. Bair and W.O. Winer, Proc. XIII Intr. Congr. Rheology (2000) 3.191.
[18} R.A. Gray, S. Chynoweth, Y. Michopoulos and G.S. Pawley, Europhysics Letters, 43(5) (1998) 491.
[19] K.P. Travis, P.J. Davis and D.J. Evans, J. Chem. Phys., 103 (1995) 10638.
[20] J. Delhommelle and D.J. Evans, J. Chem. Phys., 115 (2001) 43.
[21] E.O. Stejskal and A. Cameron, NASA Contractors Report CR-120842 (1972) 47.